Cardiac diffusion MRI beyond DTI

Valentina Mazzoli[1], Martijn Froeling[1,2], Aart J Nederveen[3], Klaas Nicolay[1], and Gustav J Strijkers[1]

[1]Biomedical NMR, Department of Biomedical Engineering, Eindhoven University of Technology, Eindhoven, Netherlands, [2]Department of Radiology, University Medical Center, Utrecht, Netherlands, [3]Department of Radiology, Academic Medical Center, Amsterdam, Netherlands

Introduction: Conventional Diffusion Tensor Imaging (DTI) has been extensively applied to study myocardial fiber architecture. DTI, however, essentially assumes a single fiber population within a voxel and a Gaussian displacement probability density function, whereas the cardiac tissue structure is significantly more complex, consisting of multiple exchanging restrictive compartments (myocytes, extracellular matrix, fibroblasts, vasculature) arranged in a complex architecture (myofibers, collagenous extracellular matrix, myolaminae).

The **aim** of this study was to investigate the consequences of non-Gaussian diffusivity and complex fiber architecture in the porcine heart by a combination of Diffusion Kurtosis Imaging (DKI) [1] and High Angular Resolution Diffusion Imaging (HARDI) with a Constrained Spherical Deconvolution (CSD) [2] analysis, in order to relate regional differences in diffusion parameters across the heart wall to the presence of the complex tissue architecture.

Acquisition: Diffusion MRI experiments were performed on *ex-vivo* pig hearts stored in 4% paraformaldehyde for at least three weeks before scanning. 24 hours before scanning the hearts were rinsed and placed in a water bath for rehydration. The data were acquired at 3T (Philips Achieva) using a twice-refocused spin-echo sequence for the complete hearts and at 9.4T (Bruker) for small heart specimens using a standard Stejskal-Tanner sequence. Multi-shot EPI readout was used for all acquisitions. DKI (3T): acquisition matrix: 144x144, voxel size: 0.97x0.97x2 mm^3, TE/TR=88/5700 ms, 3 b-values (1000, 1500, 2000 s/mm^2), Δ_1=64.22 ms, δ_1=15 ms, Δ_2=19.30 ms, δ_2=19.13 ms, 30 gradient directions and 5 b=0 images. HARDI (3T): acquisition matrix: 144x144, voxel size: 1x1x2 mm^3, TE/TR=73.5/5775 ms, b=1000 s/mm^2, Δ_1=53.6 ms, δ_1=11.47 ms, Δ_2=15.76 ms, δ_2=15.6 ms, 100 gradient directions and 11 b=0 images. HARDI (9.4T): acquisition matrix: 60x80, voxel size: 0.5x0.5x0.5 mm^3, TE/TR=18.67/12500 ms, b=1500 s/mm^2, Δ=8.5 ms, δ=4.5 ms, 100 gradient directions and 16 b=0 images.

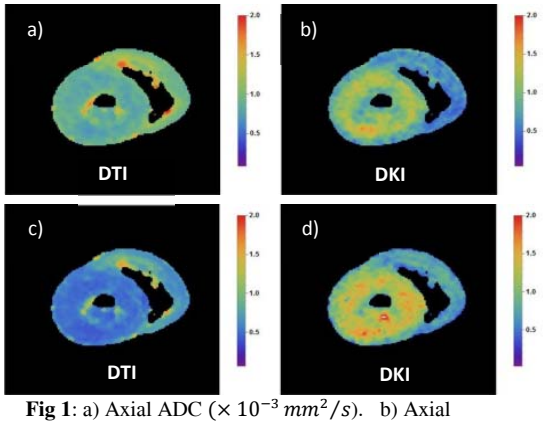

Fig 1: a) Axial ADC ($\times 10^{-3}\ mm^2/s$). b) Axial kurtosis. c) Radial ADC ($\times 10^{-3}\ mm^2/s$). d) Radial kurtosis.

Processing: All datasets were corrected for eddy current distortions and denoised using a Rician noise suppression algorithm. The DKI data were fitted to a 4th order kurtosis tensor, from which the axial and radial kurtosis were calculated. ADC maps were also calculated by fitting the data to a standard diffusion tensor model (WLLS). For the HARDI data, DTI fitting was performed, from which the threshold FA value for the response function (RF) was determined. The maximum order spherical harmonics used for CSD fitting was L_{max}=6. CSD calculation and fiber tracking were performed using ExploreDTI [3].

Results: Kurtosis maps (*Fig 1*) revealed the non-Gaussian diffusivity in the ex-vivo porcine myocardium both in the axial (parallel to local myofiber direction) and radial (perpendicular to the fibers) directions. Kurtosis was observed to be higher in the radial than in the axial direction. Interestingly, differences in the kurtosis values were observed between the right and the left ventricle, while no regional differences were observed in the corresponding ADC maps, which could be related to differences in cellularity or the more complex sheet-like arrangement (myolaminae) of the left ventricle. Indeed, CSD analysis for the complete heart at 3T (*Fig 2*) revealed an increased number of double fiber population voxels in the endocardial region of the left ventricle, when compared with the left-ventricle epicardial region and the right ventricle wall. The results of fiber tractography obtained from high resolution scans at 9.4T of a specimen of the inferior wall cut along the short axis plane is shown in *Fig 3*. The well-known double helical fiber organization was observed going from epi- to endocardium. For CSD fitting (*Fig 3b*) a second population of fibers is observed in the sub-endocardial tissue, which DTI analysis obviously failed to reveal. The two fitting methods provided the same fiber architecture in the epicardial region, where a single population of fibers was observed.

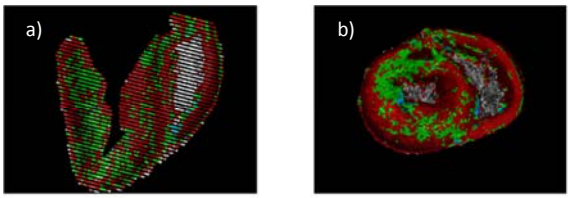

Fig 2: 3T data. CSD fitting using L_{max}=6 spherical harmonics in a) long axis view and b) basal slice in short axis view. (red=single fiber, green=double fiber population)

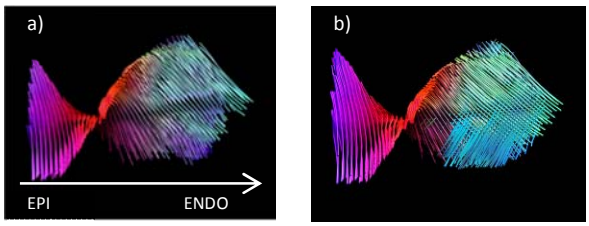

Fig 3: 9.4T data. The arrow indicates the epicardium-endocardium direction in the long axis view. Fiber tractography obtained from a) DTI fitting and b) CSD fitting using L_{max} =6. CSD revealed 2 fiber populations in the sub-endocardial tissue.

Discussions and Conclusions: Unlike DTI, the DKI method led to distinct contrast between left and right ventricle, which could be explained in terms of the higher complexity of the fiber architecture of the left ventricle, with differences in the level of cellularity and higher-order sheet-like organization. The higher kurtosis value in the radial direction as compared to axial is an indication of stronger restriction effects in the direction perpendicular to the fibers. Two fiber populations were observed using CSD in mainly the endocardial region of the left ventricular wall, which can be explained in terms of the presence of myofiber sheets (myolaminae) with different orientations. These findings are in agreement with previous histological studies [4], which showed the presence of intersecting myolaminae in the endocardial region of the left ventricle.

In summary, we have shown that DKI and CSD of the heart provide additional information with respect to standard DTI and that these two methods can be used as tools to get a deeper knowledge of cardiac microstructure non-invasively.

References: [1] Jensen et al. Magnetic Resonance in Medicine 53:1432-1440, 2005. [2] Tournier et al. Neuroimage 35:1459-1472, 2007**.** [3] www.ExploreDTI.com. [4] Gilbert et al. European Journal of Cardio-thoracic Surgery, 17:231-249, 2007.